

Final report

# Food security and social stability in Africa

New estimation methods  
for data-driven climate  
impact projections in  
data-sparse regions

---

Tamma Carleton  
Michael Greenstone  
Solomon Hsiang  
Andrew Hultgren  
Amir Jina  
Robert Kopp  
Ashwin Rode

July 2017

When citing this paper, please  
use the title and the following  
reference number:  
E-89343-INC-1

# IGC

International  
Growth Centre



DIRECTED BY



FUNDED BY



# Food Security and Social Stability in Africa: New Estimation Methods for Data-driven Climate Impact Projections in Data-sparse Regions

Tamma Carleton<sup>1</sup>, Michael Greenstone<sup>2</sup>, Solomon Hsiang<sup>1</sup>, Andrew Hultgren<sup>1</sup>, Amir Jina<sup>2</sup>, Robert Kopp<sup>3</sup>, and Ashwin Rode<sup>2</sup>

<sup>1</sup>University of California, Berkeley

<sup>2</sup>University of Chicago

<sup>3</sup>Rutgers University

July 26, 2017

## Abstract

A warming climate threatens food security and social stability in many parts of Africa. However, these locations often lack the data necessary for adequately assessing such climate risks. In this project, we develop methods to overcome this scarcity of data and obtain Africa-wide estimates of temperature sensitivities at high spatial resolution. Our approach utilizes outcomes data (on agricultural yields, conflict incidence, and crime rates) from around the world to flexibly estimate temperature sensitivities as a function of a location's adaptive capacities, which are proxied by measures of physical and socioeconomic characteristics. We generate high-resolution datasets of these measures and thereby extrapolate locally-relevant temperature sensitivities throughout Africa. We demonstrate how these estimates can be used to develop climate early warning systems by pairing our results with high-resolution seasonal climate forecasts to generate predictions of future climate-induced crime and conflict risk.

## 1 Introduction

Climate change poses an increasing threat to social stability and food security in many parts of Africa. Yet, in many of the places that are most threatened, neither existing research nor data sources exist to estimate the effect of climate on these important facets of human welfare. This represents a serious gap in both the research and policy realms. Existing empirical work that estimates climate impacts has been confined to a relatively limited subset of countries throughout the world where the requisite data are available.<sup>1</sup> While such work has provided critical insights, the extent to which these insights can be generalised to other parts of the world has never been tested. This problem is of particular concern in Africa. Because lack of data often accompanies conflict-prone and poverty-stricken locations, our knowledge of climate impacts likely ignores some of the most vulnerable locations in the world.

In this project, we develop methods to understand how climate damages shift as functions of physical and socioeconomic characteristics. Applying these methods allows us to characterize climate impact relationships in countries, sub-national regions, and even individual locations where no such research exists. In particular, our approach provides previously unknown estimates which detail climate risks and vulnerabilities across Africa, while also yielding important information on the levels of climate adaptation across locations.

These insights are the product of two major research steps. First, we assemble a large global collection of historical daily climate data and outcomes data on crime rates, conflict incidence, and agricultural yields where available. The comprehensiveness of these data allows us to flexibly estimate plausibly causal temperature responses for each outcome. Second, we account for varying levels of adaptation across locations by directly modeling spatial heterogeneity in the temperature response functions. Specifically, we allow the response functions to vary as a function of long-run

---

<sup>1</sup>A comprehensive summary of the existing work can be found in [Carleton and Hsiang \(2016\)](#).

climate (Barreca et al., 2015), income per capita (Hsiang and Narita, 2012), prevalence of irrigation (Schlenker and Roberts, 2009), and urban-ness (Burgess et al., 2014). These covariates were carefully chosen based on the literature, and new datasets were created to provide high-resolution global coverage. While the heterogeneity analysis is interesting in its own right, its key role in this study is to enable extrapolation of locally-relevant response functions to any given location, including those where outcomes data are unavailable. By inserting local values of the covariates, we map out temperature-related vulnerabilities for agricultural yields, crime, and conflict at a local level across Africa.

The rest of this report is organized as follows: Section 2 describes the data collected on outcomes, climate, and covariates; Section 3 explains the methodological innovations whereby adaptation is modeled through spatial heterogeneity in temperature responses; Section 4 applies our methods to extrapolate locally-relevant temperature responses throughout Africa; Section 5 concludes.

## 2 Data Collection

Our approach makes use of three distinct types of data: a) outcomes data on agricultural yields, crime rates, and conflict incidence; b) historical daily, as well as forecasted monthly, temperature and precipitation data; and c) data on state-level incomes, historical long-run average temperature, area equipped for irrigation, and population density. Each type of data is described in turn.

### 2.1 Outcomes Data

**Agriculture** Subnational maize production and area cropped data was collected for 43 countries with an unbalanced panel of production data spanning 1908 – 2015.<sup>2</sup> Yields were calculated as production divided by area planted where available, or divided by area harvested otherwise. Maize is calorically the most important crop in sub-Saharan Africa, accounting for approximately one-fifth of total caloric production (Cassidy et al., 2013).

**Crime and Conflict** We have collected data on the number and characteristics of both large-scale civil conflicts and interpersonal violent crimes at various spatial and temporal scales throughout the world. Guided by an extensive literature review, we have obtained the original data behind 21 distinct articles examining the link between climate and crime or conflict.<sup>3</sup>

The studies from which we have obtained data focus on a wide range of outcome variables, from civil war and ethnic riots to homicide and assault. We therefore categorize these outcomes into two groups: we call larger scale conflicts involving groups of individuals “intergroup conflict”, and smaller scale person-to-person crimes “interpersonal crime”. For intergroup conflict, we have coverage for nearly all countries in the world, although with much richer data in locations where conflict is common and heavily studied (e.g. sub-Saharan Africa). For interpersonal crime, we have subnational data for a smaller subset of countries. The geographic coverage of our data, along with spatial resolution, is shown in Figure 1.

Because our data cover diverse outcome variables at various temporal and spatial scales, we standardize both climate ( $X$ ) and outcome variables ( $Y$ ) to account for heterogeneous average levels of conflict outcomes and heterogeneous temperature variances across these different scales. Our standardized variables are defined as:

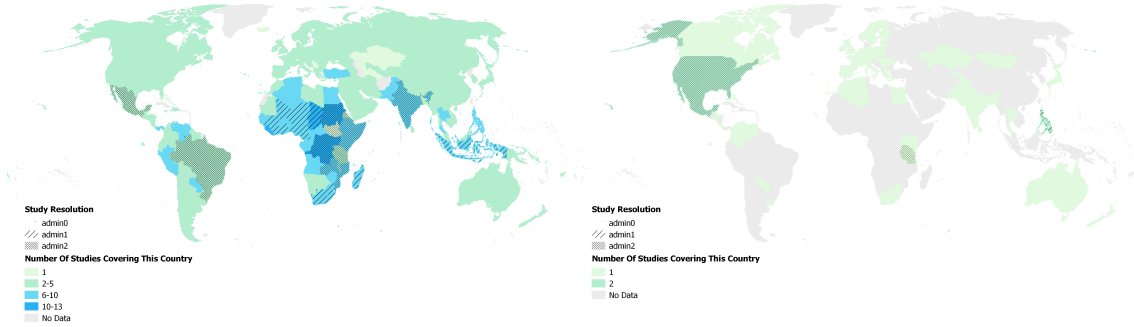
$$\check{Y}_{it} = \frac{Y_{it}}{\bar{Y}_i} \tag{1}$$

$$\check{X}_{it} = \frac{X_{it} - \bar{X}_i}{\sigma_i(X_{it})} \tag{2}$$

---

<sup>2</sup>The countries are Argentina, Brazil, Bolivia, Canada, Chile, China, Colombia, Dominican Republic, Ecuador, India, Indonesia, Mexico, Nicaragua, Nigeria, Philippines, Syria, Tanzania, Vietnam, USA, and the countries of the European Union.

<sup>3</sup>Data were sourced from the following 21 articles: Baysan et al. (2015), Bergholt and Lujala (2012), Bohlken and Sergenti (2010), Brückner and Ciccone (2011), Burke et al. (2015), Burke et al. (2009), Burke (2012), Burke and Leigh (2010), Caruso et al. (2016), Couttenier and Soubeyran (2014), Fetzer (2014), Fjelde and von Uexkull (2012), Hendrix and Salehyan (2012), Hidalgo et al. (2010), Kim (2016), Mares and Moffett (2016), Miguel (2005), Miguel et al. (2004), O’Loughlin et al. (2012), Ranson (2014), and Wetherley (2014).



(a) Intergroup conflicts

(b) Interpersonal violent crime

Figure 1: Data coverage and spatial resolution for conflict and crime

where  $Y_{it}$  and  $X_{it}$  respectively denote conflict outcome variables and climate variables observed at location  $i$  and time period  $t$ . The objects  $\bar{Y}_i$  and  $\bar{X}_i$  respectively denote the averages of  $Y$  and  $X$  at location  $i$  over all periods  $t$ , while  $\sigma_i(X_{it})$  is the standard deviation of climate variable  $X$  at location  $i$  over all periods  $t$ .

## 2.2 Climate Data

**Historical** For all sectors, we use gridded daily maximum, minimum, and/or average temperatures from two sources: The Berkeley Earth Surface Temperature (BEST) dataset, as well as the Global Meteorological Forcing Dataset for land surface modeling (GMFD) dataset. We aggregate grid cells into observations at administrative scales that match our outcome variables by taking a weighted average of the grid cells that fall within a given region. The weights used will vary by sector. In agriculture the weights are cropped area, using the Center for Sustainability and the Global Environment (SAGE) 0.1 degree gridded product, such that regional weather variables are crop-area-weighted exposure measures. For crime and conflict, we use simple area weights.

Across our outcome measures, we use distinct weather variables to capture appropriate climate exposure. These variables are summarized in Table 1. For agriculture, growing degree days (GDD) were calculated using a sinusoidal fit to daily  $T_{min}$  and  $T_{max}$  temperatures. This approach estimates a smooth fit to temperatures over time, allowing for sub-hourly measures of crop exposure to extreme temperatures and avoiding underestimating exposure to the extremes of the temperature distribution which would be associated with time-averaged measures. The GDD lower and upper breakpoints were searched for best fit to the data and set at  $0^{\circ}\text{C}$  and  $29^{\circ}\text{C}$ , respectively. "Killing degree days" (KDD) were calculated as growing degree days with a lower bound of  $29^{\circ}\text{C}$  and no upper bound, under the same sinusoidal fit to daily  $T_{min}$  and  $T_{max}$  temperatures. In conflict, we rest heavily on the expansive existing literature and use the temperature data included in each individual study from which we obtained original data, implying that our temperature variables can include both averages as well as maximum temperatures.<sup>4</sup>

In all sectors, we use gridded daily precipitation data from GMFD, or gridded monthly data from the University of Delaware, calculating appropriately-weighted regional cumulative measures of total rainfall.

**Forecasts** In this report, we demonstrate that our agricultural and conflict climate damage estimates can be effectively mobilized into a data-driven early warning system by applying our dose-response functions to short-run climate forecasts. While we show this functionality for the crime and conflict sectors here, this method is generalizable to any category of climate impacts.

A key ingredient in generating a policy-relevant forecasting tool for climate impacts is a set of climate forecasts. We use the probabilistic seasonal climate forecast product produced by the International Research Institute for Climate and Society (IRI) at Columbia University to capture

<sup>4</sup>We do not use our own temperature data because of the diversity of contexts and hence appropriate climate measures studied in these different conflict contexts. Because we standardize all analysis in conflict (see Equations 1 and 2), these differences are accounted for.

predicted temperature and rainfall distributions. These data are a re-calibration of output from NOAA’s North American Multi-Model Ensemble Project (NMME), and the output is provided on a 1 degree grid at the global scale. We convert these probabilistic forecasts into z-scores of temperature (for temperature exposure measures) and levels of precipitation (as a control), and spatially aggregate these forecasts into regional metrics that can be used as inputs into hyper-local climate impact estimation.

### 2.3 Covariate Data

Data on the following covariates are used to explain spatial heterogeneity in the temperature responses of the outcomes. Exact details on how the covariates are constructed for each outcome can be found in Table 2.

**Temperature** Historical long-run average temperature is calculated from the temperature datasets used in the analysis and described above. The average is taken over the years that correspond to the outcome data. This is calculated at the 1<sup>st</sup>-level administrative division (i.e. ADM1) in order to match the level at which the administrative income data is available. For country-level outcome data, we use country-level long-run average temperatures.

**Sub-national Incomes** Sub-national incomes measured in constant 2005 dollars adjusted for purchasing power parity (PPP) are obtained from [Gennaioli et al. \(2012\)](#), which reports sub-national incomes gathered from administrative data around the world. These data are typically not annual, and are drawn from census data. We match incomes in the cross-section to ADM1 units in our sample based on the sample period for each country. For country-level outcome data, we use World Bank income data, also in constant 2005 dollars and PPP-adjusted.

**Area Equipped for Irrigation** To measure the cropland area equipped for irrigation (AEI), we used the Global Map of Irrigated Areas from [Siebert et al. \(2013\)](#), which shows the percentage of grid cell area equipped for irrigation around the year 2005. The Global Map of Irrigated Areas is provided at 5 minute grid cells.

**Population density** Population density is derived from Landsat. We use this high-resolution gridded dataset to create a measure of urban-ness, distinct from population density in an administrative region. As average population density across any of our regions is highly dependent on the value of area in the denominator, this measure will not capture how urban an area is. This is particularly true in cases where large administrative regions comprise unpopulated desert and highly concentrated urban centers. We transform this into a measure of urban-ness by calculating the population-weighted population density, or the population density that *an average person perceives* in an administrative region.

## 3 Methodological Innovations

Our method involves 3 steps. We first estimate a dose-response relationship between temperature and each outcome using all available global data for that outcome. Second, we explore how this relationship varies across locations. Spatial (i.e. cross-sectional) heterogeneity in the dose-response relationship is empirically modeled as a function of location-specific factors, which, depending on the outcome, may include per-capita GDP, long-run temperature, and percent of cropped area that is irrigated. These covariates are meant to capture dimensions along which adaptation to extreme temperatures might occur. The third step consists of extrapolation based on the heterogeneity estimates. By inserting the appropriate values of the covariates, a dose-response relationship, reflective of adaptive capabilities, can be characterized for any location, including those lacking data on the underlying outcome.

### 3.1 Step 1: Dose-response Function Estimation

The global dose-response function flexibly models the relationship between temperature in degrees Celsius ( $T$ ) and outcome ( $Y$ ). Each outcome variable is measured for some unit  $i$  at time  $t$ , with

the set of outcomes and their spatial and temporal resolutions detailed in Table 1. The explanatory variable of interest (i.e. temperature) is modeled through a (possibly) non-linear function  $f(T)$ .

The regression specifications take the following general form:

$$Y_{i,t} = f(T_{i,t}) + Controls_{i,t} + FixedEffects + \varepsilon_{it}. \quad (3)$$

The exact form for the function  $f$  varies by outcome, as do the control variables and fixed effects. The particulars for each outcome are listed in Table 1. The variable  $\varepsilon_{it}$  denotes the remaining idiosyncratic error.

For the agricultural yield outcome, the response at any given temperature is expressed as the difference between the predicted yield at that temperature and the predicted yield at a reference temperature ( $T_{ref}$ ) of 29°C.<sup>5</sup> For example, the response of yield on a day where the temperature is  $x$  degrees Celsius is:

$$Response(x) = f(x) - f(29) \quad (4)$$

For the crime and conflict outcomes, the estimation employs a temperature exposure measured in z-scores. Therefore, the function  $f$  itself captures a response that is relative to the sample average temperature. Thus, the estimated predicted response of these outcomes at a temperature z-score  $x$  is simply  $Response(x) = f(x)$ .

In the next step, we exploit data on location-specific covariates to model how differential adaptation affects the shape of the response function.

### 3.2 Step 2: Interpolation Surface Estimation

The outcomes data necessary to directly estimate equation (3) are available only for a limited number of countries, posing a challenge for conducting globally valid climate impact analyses. In order to address this issue, we develop a model of interactions to characterize heterogeneity in the response. Specifically, we augment equation (3) to include interactions between temperature and other factors (i.e. location-specific covariates) at the first administrative level (i.e. state or province) for subnational data, and at the national level for country data. The factors are as follows, with the exact interactions described in Table 2:

1. *Income* measured as the natural log of per-capita GDP over some representative year(s). See Table 2 for the years used for each outcome.
2. *Long – run temperature* measured for each outcome as described in Table 2.
3. *Percent cropped area irrigated* (for agricultural yield outcome only).
4. *Population density* (for crime and conflict only), measured as the natural log of population density in the year 2000.

We chose these factors because they plausibly capture differential adaptive responses across locations. Prior literature has emphasized the adaptive significance of average climate (Barreca et al., 2015), income per-capita (Hsiang and Narita, 2012), urban-ness (Burgess et al., 2014), and, for agricultural yields, irrigation (Schlenker and Roberts, 2009). For example, higher per-capita GDP entails greater capability to invest in adaptive goods and services. Furthermore, the dose-response relationship may also depend on long-run exposure to extreme temperatures as places with greater previous exposure may differ in their adaptive behaviors. Additionally, irrigation may mitigate the harmful effects of extreme temperatures on agriculture yields.

For each outcome, we parameterize the heterogeneity in the function  $f(T)$  due to the factors (see Table 2 for specific parameterizations by outcome), and thereby estimate  $f(T)$  as conditional on the factors. Letting  $\mathbf{z}$  denote the vector of factors, the conditional function is thus  $f(T|\mathbf{z})$ . Estimating the object  $f(T|\mathbf{z})$  paves the way for the third step of the analysis— predicting dose-response values at a local level.

---

<sup>5</sup>In other words, the response to a temperature of 29°C is normalized to zero.

Table 1: Dose-Response Estimation by Sector

Outcome	Spatial Resolution	Temporal Resolution	Functional Form	Fixed Effects	Controls	$T_{ref}$
Yield	District (Adm2)	Annual	Piecewise linear, Sinusoidal intraday fit	District, country-year	Quadratic precipitation	29° C
Violent Crime Incidence	Various (grid cell to country)	Various (daily-annual)	Linear in z-score of original study temperature exposure	Study $\times$ region, study $\times$ region $\times$ month, study $\times$ year	Quadratic precipitation	N/A
Conflict Incidence	Various (grid cell to country)	Various (monthly-annual)	Linear in z-score of original study temperature exposure	Study $\times$ region, study $\times$ region $\times$ month, study $\times$ year	Quadratic precipitation	N/A

“Region” refers to the spatial resolution of the observation (e.g. county, state, country).

Table 2: Factor Interactions by Sector

Outcome	Income	Long-run Temperature	Other Covariate
Yield	$\log(GDP_{pc})$ in year of observation <sup>a</sup>	Growing season average $T_{max}$ in sample period	Cropland share irrigated
Violent Crime Incidence	$\log(GDP_{pc})$ in sample period <sup>a</sup>	Average annual temperature in sample period	$\log(popdens)$ in sample period
Conflict Incidence	$\log(GDP_{pc})$ in sample period <sup>a</sup>	Average annual temperature in sample period	$\log(popdens)$ in sample period

<sup>a</sup> Subnational income data are linearly interpolated between the years provided in [Gennaioli et al. \(2012\)](#).

### 3.3 Step 3: Interpolating Dose-response Relations

Estimating  $f(T|\mathbf{z})$  makes it possible to interpolate a response function to any location of the world where the values of the covariates are known. We predict dose-response values at the *impact region* level throughout Africa, where we have created data to identify the values of each factor. *Impact regions* are a set of boundaries created by us for the purpose of extrapolating temperature sensitivities derived from our estimation. Impact regions are constructed such that they are identical to existing administrative regions or are a union of a small number of administrative regions.<sup>6</sup> There are 3400 impact regions in Africa, the boundaries of which are depicted in Figure 2.



Figure 2: Impact Regions in Africa

<sup>6</sup>We use the Global Administrative Region dataset ([Global Administrative Areas, 2012](#)) to delineate boundaries for impact regions, but require fewer than the approximately 295,000 spatial units present in that dataset. We therefore agglomerate the spatial units to create a set of 24,378 impact regions globally that allow for greater comparability and computational feasibility than unagglomerated regions. We establish a set of criteria to create these regions that makes them approximately comparable across regions with respect to population, and internally consistent with respect to mean temperature, diurnal temperature range, and mean precipitation.

To obtain per-capita income at the impact region level, we allocate national GDP based on the impact region’s mean frequency of nightlights between 1992 and 2013 (Henderson et al., 2012).<sup>7</sup> All other factors are obtained at the impact region level by aggregating gridded data from the sources described in Section 2.3.

Formally, the estimated, predicted response for agricultural yield at a temperature  $x$  (relative to 29°C) in an impact region with covariate vector  $\mathbf{z}_i$  is:

$$Response(x|\mathbf{z}_i) = f(x|\mathbf{z}_i) - f(29|\mathbf{z}_i). \quad (5)$$

For the crime and conflict outcomes, which are estimated using a z-score measure of temperature exposure, the estimated predicted response at a temperature z-score  $x$  in an impact region with covariate vector  $\mathbf{z}_i$  is simply  $Response(x|\mathbf{z}_i) = f(x|\mathbf{z}_i)$ .

In the next section, we map these estimates of predicted responses for each outcome at extreme temperature values.

## 4 Applications

To demonstrate the application of our methodological innovations, we explore the local impacts of high temperature days on each outcome throughout Africa. The subsequent maps illustrate impacts that reflect adaptive capabilities (i.e. income, long-run temperature, irrigation, and urban-ness) as of 2010.

### 4.1 Agriculture

In estimating the maize response surface, we find two forms of climate adaptation. Farms that are more frequently exposed to extreme heat, measured via exposure to long-run  $T_{max}$ , exhibit a muted negative response of yields to extreme heat shocks. Likewise, high levels of irrigation also mute the adverse effects of extreme heat shocks, presumably through directly cooling crops and reducing the water-stress effects of extreme heat.

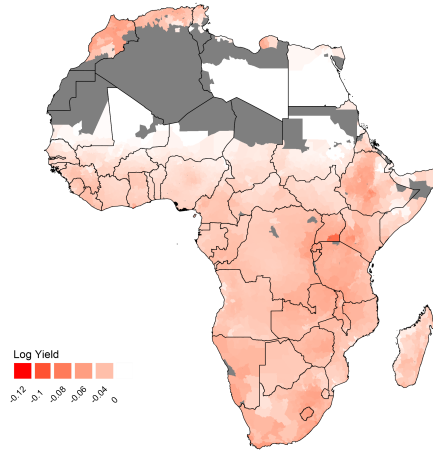
The maize response surface was interpolated for all of SSA using impact area covariate data, as described previously.<sup>8</sup> The results of this interpolation are displayed in Figure 3. The first chart depicts the yield loss (in log points) associated with 24 hours of constant exposure to a temperature of 35°C, relative to the yield at the estimated optimal maize growing temperature of 29°C. These are the projected responses, allowing for the adaptive effects of climate adaptation and irrigation described above. So, a value of -0.03 would indicate a 3% yield loss relative to the ideal maize temperature, conditional on the long-run climate and current level of irrigation in any given impact region. Regions with a lesser estimated yield loss will have higher levels of irrigation and/or higher levels of long-run  $T_{max}$ . The second chart in Figure 3 is identical to the first, except the exposure depicted is for 24 hours of constant temperature at 40°C, instead of 35°C.

It should be noted that these effects, as modeled, are additive. Take, for example, a region which is estimated to exhibit a 10% loss of yields under exposure to 24 hours of 40°C temperatures. If that region is exposed to 72 hours of 40°C temperatures over the course of a growing season, yield losses will be projected to be 30% on average, relative to the counterfactual of optimal growing temperature during those 72 hours.

<sup>7</sup>Specifically, we first estimate a linear relationship between the z-score of GDP per capita and z-score of nightlight frequency for the sample of US counties in 2011, where both these variables are available. We then apply these coefficient estimates to nightlights density measurements to predict GDP per capita at the impact region level in other countries.

<sup>8</sup>The maize response surface to KDD was clipped at zero. In the unclipped surface, some areas of southern Egypt, northern Sudan, southern Libya, and northern Mali were predicted to have a slightly positive response to extreme heat shocks in the interpolated surface. These arid regions have extremely high values of long-run  $T_{max}$  and have limited (if any) maize production, so we believe clipping is justified in this case.

Change in Log Maize Yields  
from 24hrs at 35C



Change in Log Maize Yields  
from 24hrs at 40C

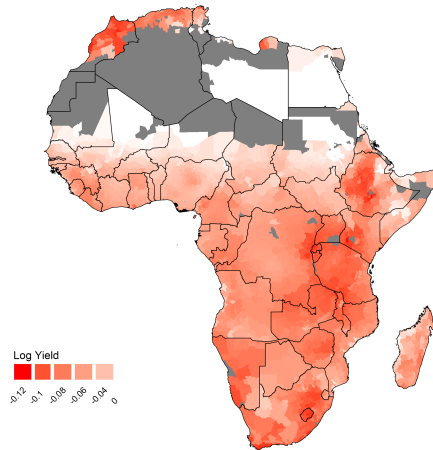


Figure 3: Maize response interpolation for impact regions in SSA. The first chart depicts the yield loss (in log points) associated with 24 hours of constant exposure to a temperature of 35°C, relative to the yield at the estimated optimal maize growing temperature of 29°C. The second chart depicts the same, except for 24 hours of constant exposure to a temperature of 40°C. The maize response surface to KDD was clipped at zero.

## 4.2 Crime and Conflict

For interpersonal crime and intergroup conflict independently, we use the interpolation method described above to generate predicted temperature sensitivities throughout India. The results of this interpolation are displayed in Figure 4. In panel (a), the map shows the predicted increase in civil conflict incidence caused by a one standard deviation increase in temperature exposure. In panel (b), the map shows the same value, but for interpersonal violent crime. Note that as above for agricultural yields, these are the projected responses, allowing for the adaptive effects of climate adaptation and income described above.

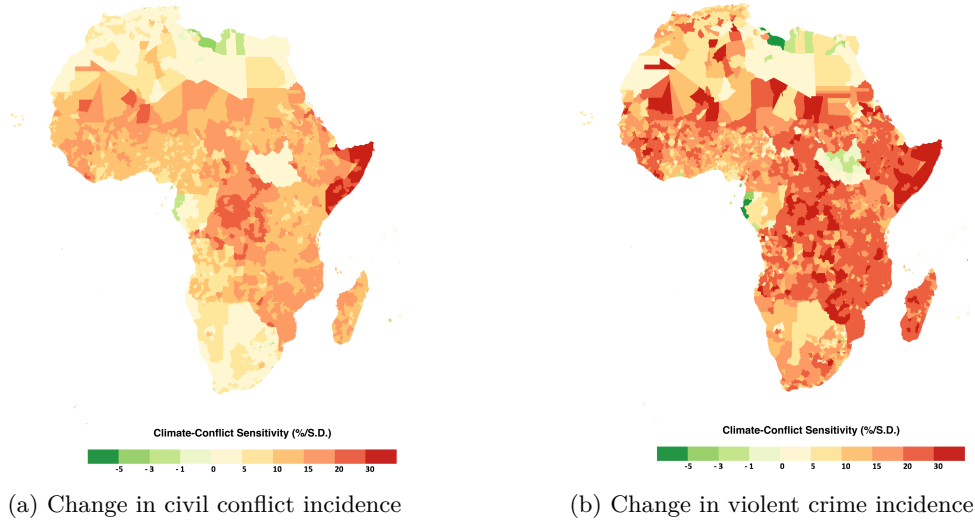


Figure 4: Impact of temperature on crime and conflict. Panel (a) depicts the % change in conflict per standard deviation ( $\sigma$ ) increase in temperature, where temperature exposure is defined using a range of variables, from monthly maximum temperature to annual average temperature. Panel (b) shows the same results, but for interpersonal violent crimes.

Across all of Africa, the average baseline number of annual conflicts per country is 580, according to the Armed Conflict Location and Event Data Project (ACLED). Our estimates shown in panel (a) of Figure 4 predict that a one standard deviation increase in temperature will cause an additional 64 conflicts per country per year; this corresponds to an average effect of an 10.8% increase in conflict per standard deviation increase in temperature, although this average masks substantial spatial heterogeneity shown in panel (a).

While both interpersonal crimes and larger scale civil conflicts tend to increase with warming temperatures, the magnitudes of these effects and their spatial patterns have been shown to differ substantially (Burke et al., 2015). Consistent with this previous evidence, we find that predicted temperature sensitivities for interpersonal crime exhibit distinct behavior to those estimated for intergroup conflict. The interpolation results for crime are shown in panel (b) of Figure 4. As for intergroup conflict, the map in panel (b) shows the predicted increase in violent crime incidence caused by a one standard deviation increase in temperature exposure. Across all of Africa, we predict that the average effect of a one standard deviation increase in temperature exposure is 16.2% for violent crime, a significantly higher average value than that for intergroup conflict. Applying this estimate to the case of homicides, we estimate that the average number of homicides per year per country, currently at 11.7 per 100,000 (Mares and Moffett, 2016), will rise by 1.45 per 100,00 in response to a one standard deviation increase in temperature. While similar, the spatial pattern of these deaths is distinct from that shown in panel (a); for both interpersonal crime and for intergroup conflict, the highest sensitivity locations are the relatively poor, central regions.

Together, these findings demonstrate how our methodology can harness large amounts of diversely-collected data to generate hyper-local predictions of climate impacts. In particular, these crime and conflict climate impact maps have the potential to be exceptionally valuable to policymakers responsible for preventing and combating outbreaks of violence which may be linked to fluctuations in the climate. To demonstrate this functionality, in the next section we combine these hyper-localized temperature sensitivities with seasonal climate forecasts to generate short-run forecasts of crime and conflict on scales directly relevant to policymakers.

**Forecasted impacts** Using the interpolated temperature sensitivities described above, in combination with analogous precipitation sensitivities estimated for precipitation, we generate short-run forecasts of crime and conflict incidence by relying on the IRI seasonal climate forecast data. These results are shown below in Figure 5.

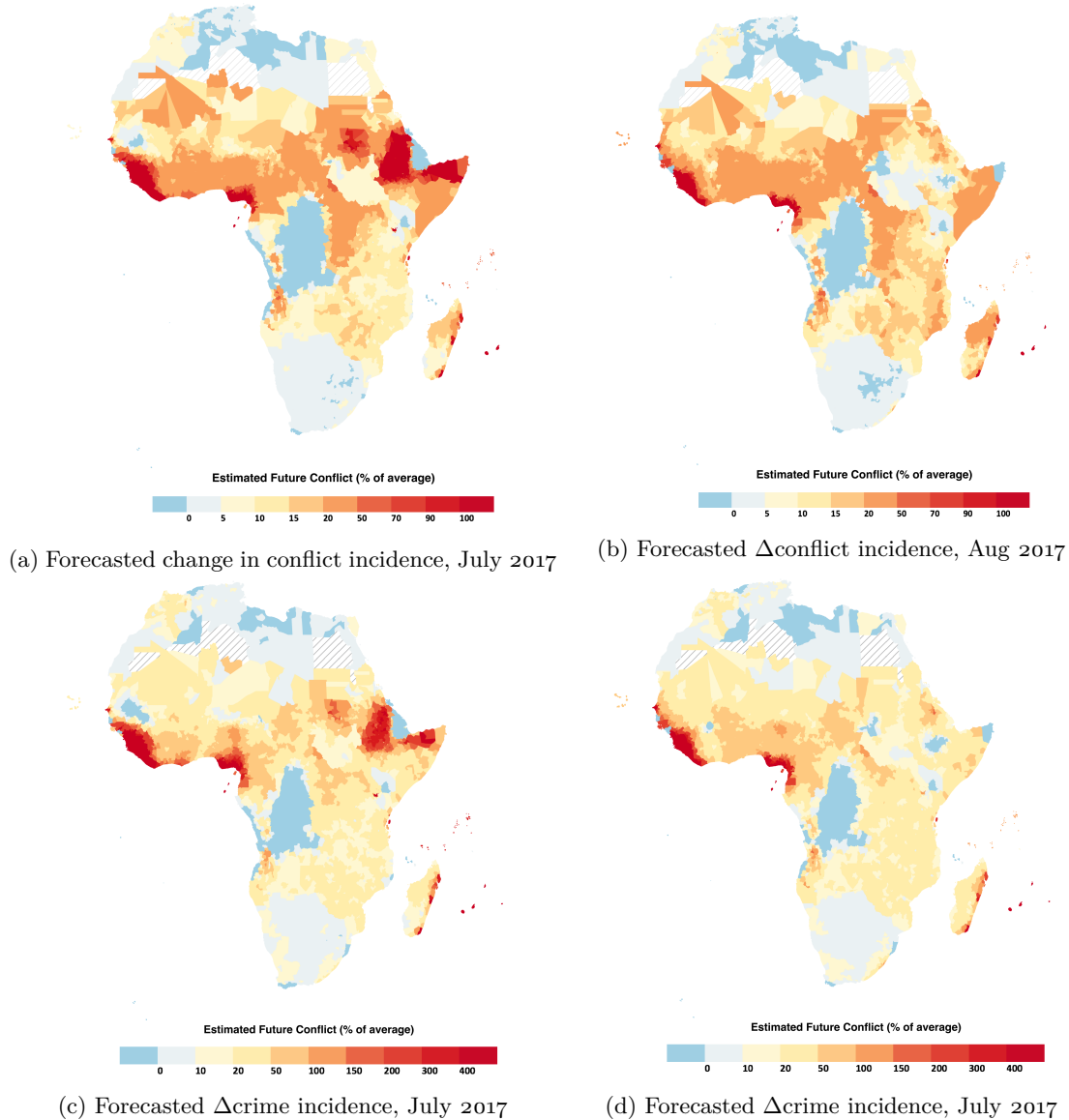


Figure 5: Forecasted Impact of Heat on Civil Conflict and Violent Crime. Each panel depicts the change in conflict or crime incidence relative to the average level. (Dashed areas indicate locations where the IRI climate forecasts are missing data.)

These results provide a user-friendly window into data-driven climate impact estimation, providing stakeholders with maps at high spatial and temporal resolution indicating the regions of immediate concern for intergroup, interpersonal, or both types of crime and conflict.

## 5 Conclusion

Although Africa includes some of the most climate-vulnerable areas in the world, the lack of data has hampered efforts to assess climate impacts in these locations. The methodological innovations of this project are designed to overcome this paucity of data and yield unprecedented, hyper-local insights into climate risks for two important facets of human welfare— food security and social stability.

Our approach utilizes outcomes data (i.e. data on agricultural yields, conflict incidence, and crime rates) from around the world to flexibly estimate temperature sensitivities as a function of a location's adaptive capacities, which we model through measures of income, long-run climate, irrigation, and urban-ness. We have developed high-resolution, global datasets of these measures, thus making it possible to extrapolate locally-relevant temperature sensitivities at any given location.

Our findings suggest that extreme heat exposure leads to substantial losses in maize yields throughout most of sub-Saharan Africa. For instance, twenty-four hours of exposure to a temperature of  $40^{\circ}\text{C}$  results in yield losses of up to 12 percent (depending on location), relative to the yield at the estimated optimal maize growing temperature of  $29^{\circ}\text{C}$ . Some of the worst affected areas include the relatively poor, central regions. Crime and conflict are also seen to increase with exposure to warmer temperatures. A one standard deviation increase temperature is expected to cause a 10.8% average increase in conflict incidence and 16.2% average increase in the violent crime rate, however both these averages mask considerable spatial heterogeneity. As with maize yields, some of the worst affected areas include the central regions.

In addition to shedding light on future climate vulnerability, the methods developed in this project also have the potential to be used as a near-term forecasting tool. We demonstrate an example of this for the crime and conflict outcomes. Such a tool can equip policymakers with valuable information for better allocating scarce resources to areas of immediate concern.

## References

- A. Barreca, K. Clay, O. Deschênes, M. Greenstone, and J. S. Shapiro. Convergence in adaptation to climate change: Evidence from high temperatures and mortality, 1900–2004. *The American Economic Review*, 105(5):247–251, 2015.
- C. Baysan, M. Burke, F. Gonzalez, S. Hsiang, and E. Miguel. Economic and non-economic factors in violence: Evidence from organized crime, suicides and climate in mexico. *Department of Agricultural and Resource Economics, University of California, Berkeley*, 2015.
- D. Bergholt and P. Lujala. Climate-related natural disasters, economic growth, and armed civil conflict. *Journal of Peace Research*, 49(1):147–162, 2012.
- A. T. Bohlken and E. J. Sergenti. Economic growth and ethnic violence: An empirical investigation of hindu—muslim riots in india. *Journal of Peace research*, 47(5):589–600, 2010.
- M. Brückner and A. Ciccone. Rain and the democratic window of opportunity. *Econometrica*, 79(3):923–947, 2011.
- R. Burgess, O. Deschenes, D. Donaldson, and M. Greenstone. The unequal effects of weather and climate change: Evidence from mortality in india. *Cambridge, United States: Massachusetts Institute of Technology, Department of Economics. Manuscript*, 2014.
- M. Burke, S. M. Hsiang, and E. Miguel. Climate and conflict. *Annu. Rev. Econ.*, 7(1):577–617, 2015.
- M. B. Burke, E. Miguel, S. Satyanath, J. A. Dykema, and D. B. Lobell. Warming increases the risk of civil war in africa. *Proceedings of the national Academy of sciences*, 106(49):20670–20674, 2009.
- P. J. Burke. Economic growth and political survival. *The BE Journal of Macroeconomics*, 12(1), 2012.
- P. J. Burke and A. Leigh. Do output contractions trigger democratic change? *American Economic Journal: Macroeconomics*, 2(4):124–157, 2010.
- T. A. Carleton and S. M. Hsiang. Social and economic impacts of climate. *Science*, 353(6304):aad9837, 2016.
- R. Caruso, I. Petrarca, and R. Ricciuti. Climate change, rice crops, and violence: Evidence from indonesia. *Journal of Peace Research*, 53(1):66–83, 2016.
- E. S. Cassidy, P. C. West, J. S. Gerber, and J. A. Foley. Redefining agricultural yields: from tonnes to people nourished per hectare. *Environmental Research Letters*, 8(3):034015, 2013.
- M. Couttenier and R. Soubeyran. Drought and civil war in sub-saharan africa. *The Economic Journal*, 124(575):201–244, 2014.
- M. Dell, B. F. Jones, and B. A. Olken. Temperature shocks and economic growth: Evidence from the last half century. *American Economic Journal: Macroeconomics*, 4(3):66–95, 2012.
- T. Fetzer. Can workfare programs moderate violence? evidence from india. 2014.
- H. Fjelde and N. von Uexkull. Climate triggers: Rainfall anomalies, vulnerability and communal conflict in sub-saharan africa. *Political Geography*, 31(7):444–453, 2012.
- N. Gennaioli, R. La Porta, F. Lopez-de Silanes, and A. Shleifer. Human capital and regional development. *The Quarterly journal of economics*, 128(1):105–164, 2012.
- Global Administrative Areas. Gadm database of global administrative areas, version 2.0. *URL: <http://www.gadm.org> [accessed 201–03–24]*, 2012.
- J. V. Henderson, A. Storeygard, and D. N. Weil. Measuring economic growth from outer space. *The American Economic Review*, 102(2):994–1028, 2012.

- C. S. Hendrix and I. Salehyan. Climate change, rainfall, and social conflict in africa. *Journal of peace research*, 49(1):35–50, 2012.
- F. D. Hidalgo, S. Naidu, S. Nichter, and N. Richardson. Economic determinants of land invasions. *The Review of Economics and Statistics*, 92(3):505–523, 2010.
- S. M. Hsiang and D. Narita. Adaptation to cyclone risk: Evidence from the global cross-section. *Climate Change Economics*, 3(02):1250011, 2012.
- N. K. Kim. Revisiting economic shocks and coups. *Journal of Conflict Resolution*, 60(1):3–31, 2016.
- D. M. Mares and K. W. Moffett. Climate change and interpersonal violence: a “global” estimate and regional inequities. *Climatic change*, 135(2):297–310, 2016.
- E. Miguel. Poverty and witch killing. *The Review of Economic Studies*, 72(4):1153–1172, 2005.
- E. Miguel, S. Satyanath, and E. Sergenti. Economic shocks and civil conflict: An instrumental variables approach. *Journal of political Economy*, 112(4):725–753, 2004.
- J. O’Loughlin, F. D. Witmer, A. M. Linke, A. Laing, A. Gettelman, and J. Dudhia. Climate variability and conflict risk in east africa, 1990–2009. *Proceedings of the National Academy of Sciences*, 109(45):18344–18349, 2012.
- M. Ranson. Crime, weather, and climate change. *Journal of environmental economics and management*, 67(3):274–302, 2014.
- W. Schlenker and M. J. Roberts. Nonlinear temperature effects indicate severe damages to us crop yields under climate change. *Proceedings of the National Academy of sciences*, 106(37):15594–15598, 2009.
- S. Siebert, V. Henrich, K. Frenken, and J. Burke. Update of the digital global map of irrigation areas to version 5. *Rheinische Friedrich-Wilhelms-Universität, Bonn, Germany and Food and Agriculture Organization of the United Nations, Rome, Italy*, 2013.
- E. Wetherley. Typhoons and temperature impact crime rates: evidence from the philippines. 2014.

The International Growth Centre (IGC) aims to promote sustainable growth in developing countries by providing demand-led policy advice based on frontier research.

Find out more about our work on our website  
[www.theigc.org](http://www.theigc.org)

---

For media or communications enquiries, please contact  
[mail@theigc.org](mailto:mail@theigc.org)

---

Subscribe to our newsletter and topic updates  
[www.theigc.org/newsletter](http://www.theigc.org/newsletter)

---

Follow us on Twitter  
[@the\\_igc](https://twitter.com/the_igc)

---

Contact us  
International Growth Centre,  
London School of Economic and Political Science,  
Houghton Street,  
London WC2A 2AE

**IGC**

**International  
Growth Centre**

DIRECTED BY



FUNDED BY



Designed by [soapbox.co.uk](http://soapbox.co.uk)